

Fractional–Order Oscillator Based on Single CCII

Lobna A. Said^a, Ahmed G. Radwan^{b,c}, Ahmed H. Madian^{c,d}, Ahmed M. Soliman^e

^a Faculty of IET, German University in Cairo (GUC), Egypt. Email: l.a.said@ieee.org

^bDept. of Engineering Mathematics and Physics, Cairo University, Egypt. Email: agradwan@ieee.org

^cNISC Research Center, Nile University, Cairo, Egypt

^dRadiation Engineering Dept., NCRRT, Egyptian Atomic Energy, Authority. Email: dr.ahmed.madian@ieee.org

^eElectronics and comm. Eng. Dept., Cairo University, Egypt. Email: asoliman@ieee.org

Abstract—This paper presents a generalization of well-known phase shift oscillator based on single CCII into the fractional order domain. The general state matrix, characteristic equation and design equations are presented. The general oscillation frequency, condition and the phase difference between the oscillatory outputs are introduced in terms of the fractional order parameters. These parameters add extra degrees of freedom which in turn increase the design flexibility and controllability. Numerical discussion of five special cases is investigated including the integer case. Spice simulations and experimental results are introduced to validate the theoretical findings with stability discussion.

Keywords—Fractional calculus; oscillators; CCII

I. INTRODUCTION

The second generation current conveyor (CCII) depicted in Fig. 1(a) is a current mode active device which was first introduced by Sedra [1]. It is a three port network where its terminal characteristics can be described by the following matrix [1-2]:

$$\begin{bmatrix} I_Y \\ V_X \\ I_Z \end{bmatrix} = \begin{bmatrix} 0 & 0 & 0 \\ 1 & 0 & 0 \\ 0 & \pm 1 & 0 \end{bmatrix} \begin{bmatrix} V_Y \\ I_X \\ V_Z \end{bmatrix}, \quad (1)$$

where V_X, V_Y, V_Z, I_X, I_Y , and I_Z are the voltages and the currents of X-, Y-, and Z- terminals respectively. The Y- terminal has high input impedance suitable for input voltage while the X-terminal has low input impedance suitable for input current. The implementation of the CCII- by the AD844 chip for experimental purposes is depicted in Fig. 1(b). The CCII has been used in many applications including oscillators and filters as presented in [2-5].

The fractional calculus is the generalization of the conventional integration and differentiation to non-integer orders [6]. It was known centuries ago. However, it was far from application point of view till the early sixties where it has great contributions in science and engineering [7-14]. It gives extra degree of freedom which is the order of the derivative or integral; it increases the flexibility of the design and it adds more fundamentals. Lots of theories are evolved due to these new fundamentals such as the theory of fractional order oscillators. The theory of fractional order oscillators with three fractance devices was presented in [8-9]. It states that a linear fractional order system of the form described by:

$$\begin{bmatrix} D^\alpha v_1 \\ D^\beta v_2 \\ D^\gamma v_3 \end{bmatrix} = \begin{bmatrix} a_{11} & a_{12} & a_{13} \\ a_{21} & a_{22} & a_{23} \\ a_{31} & a_{32} & a_{33} \end{bmatrix} \begin{bmatrix} v_1 \\ v_2 \\ v_3 \end{bmatrix} = [A] \begin{bmatrix} v_1 \\ v_2 \\ v_3 \end{bmatrix}, \quad (2)$$

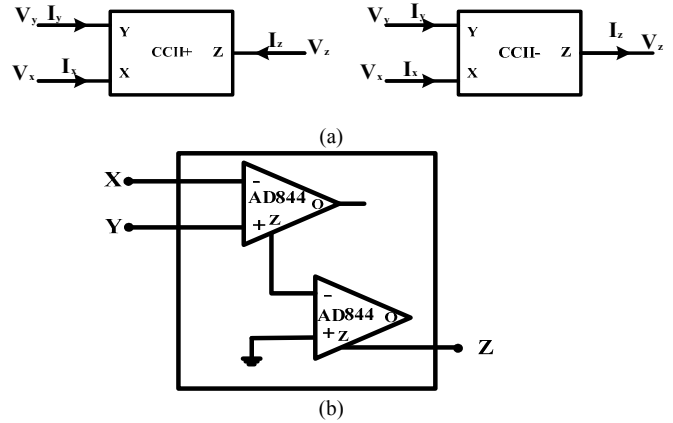


Fig. 1. (a) CCII block diagram, and (b) CCII- implementation with AD844.

achieves sinusoidal oscillations if there exists a value for ω to satisfy the following equation:

$$\begin{aligned} & \omega^{\alpha+\beta+\gamma} \cos\left(\frac{(\beta+\alpha+\gamma)\pi}{2}\right) + \omega^\beta |A_\beta| \cos\left(\frac{\beta\pi}{2}\right) + \\ & \omega^\alpha |A_\alpha| \cos\left(\frac{\alpha\pi}{2}\right) + \omega^\gamma |A_\gamma| \cos\left(\frac{\gamma\pi}{2}\right) - \\ & a_{11} \omega^{\beta+\gamma} \cos\left(\frac{(\gamma+\beta)\pi}{2}\right) - a_{22} \omega^{\alpha+\gamma} \cos\left(\frac{(\alpha+\gamma)\pi}{2}\right) - \\ & a_{33} \omega^{\alpha+\beta} \cos\left(\frac{(\alpha+\beta)\pi}{2}\right) - |A| = 0, \end{aligned} \quad (3a)$$

$$\begin{aligned} & \omega^{\alpha+\beta+\gamma} \sin\left(\frac{(\beta+\alpha+\gamma)\pi}{2}\right) + \omega^\beta |A_\beta| \sin\left(\frac{\beta\pi}{2}\right) + \\ & \omega^\alpha |A_\alpha| \sin\left(\frac{\alpha\pi}{2}\right) + \omega^\gamma |A_\gamma| \sin\left(\frac{\gamma\pi}{2}\right) - \\ & a_{11} \omega^{\beta+\gamma} \sin\left(\frac{(\gamma+\beta)\pi}{2}\right) - a_{22} \omega^{\alpha+\gamma} \sin\left(\frac{(\alpha+\gamma)\pi}{2}\right) - \\ & a_{33} \omega^{\alpha+\beta} \sin\left(\frac{(\alpha+\beta)\pi}{2}\right) = 0. \end{aligned} \quad (3b)$$

where $|A_\alpha| = a_{22}a_{33} - a_{23}a_{32}$, $|A_\beta| = a_{11}a_{33} - a_{13}a_{31}$, and $|A_\gamma| = a_{11}a_{22} - a_{12}a_{21}$. The transfer function (TF) between the states in s-domain is important to find the phase difference between them.

Recently, many papers were introduced to generalize the integer-order oscillator designs into the fractional order domain [8-11]. A generalization of a family of OTRA based oscillators was presented in [10] where the general oscillation frequency, condition and the phase difference were investigated. A general analysis of the generation for all possible fractional order oscillators based on two port network was presented in [11].

The aim of this work is to generalize a well-known phase shift oscillator into the fractional-order domain. The generalization process is done through replacing the integer order capacitors with fractional order ones. The fractional order

capacitor depicted in Fig.2 has the impedance $(s) = 1/(s^\alpha c)$, where $0 < \alpha < 1$. The conventional capacitor could be considered as special case from the general fractional order capacitor. The implementation of the fractional order capacitor into a feasible device was investigated in [12, 13]. For $\alpha > 1$, the fractional order capacitor can be realized with the generalized impedance converter (GIC)[14].

This paper is organized as follows; section II discusses the oscillator structure, the general design equations with numerical discussion of some special cases. Section III illustrates Spice simulation, experimental results and stability discussion for different cases and finally section IV concludes the work.

II. OSCILLATOR STRUCTURE AND DISCUSSION

The oscillator depicted in Fig.3 is the generalization of phase shift oscillator presented in [2]. The oscillator consists of one CCII with three fractional order capacitors and three resistors. The general state matrix describes this oscillator is written as follows:

$$\begin{bmatrix} D^\alpha v_1 \\ D^\beta v_2 \\ D^\gamma v_3 \end{bmatrix} = \begin{bmatrix} -1 & 1 & 0 \\ CR & CR & -2 \\ 1 & -2 & 1 \\ CR & CR & CR \\ -1 & 1 & -1 \\ CR_3 & CR & CR \end{bmatrix} \begin{bmatrix} v_1 \\ v_2 \\ v_3 \end{bmatrix}. \quad (4)$$

The characteristic equation of this oscillator based on the previous state matrix can be described as follows:

$$s^{\alpha+\beta+\gamma} + \frac{s^{\beta+\alpha}}{CR} + \frac{s^{\beta+\gamma}}{CR} + \frac{2s^{\alpha+\gamma}}{CR} + \frac{s^\beta}{R^2C^2} + \frac{s^\alpha}{R^2C^2} + \frac{s^\gamma}{R^2C^2} + \frac{1}{C^3R^2R_3} = 0. \quad (5)$$

According to the general fractional-order oscillator theory, the circuit will oscillate if there is value for ω satisfies the following:

$$\frac{\omega^{\alpha+\beta+\gamma} \cos\left(\frac{(\beta+\alpha+\gamma)\pi}{2}\right) + \frac{\omega^{\beta+\alpha} \cos\left(\frac{(\beta+\alpha)\pi}{2}\right)}{CR} + \frac{\omega^{\beta+\gamma} \cos\left(\frac{(\gamma+\beta)\pi}{2}\right)}{2\omega^{\alpha+\gamma} \cos\left(\frac{(\alpha+\gamma)\pi}{2}\right) + \frac{\omega^\beta \cos\left(\frac{\beta\pi}{2}\right)}{R^2C^2} + \frac{\omega^\alpha \cos\left(\frac{\alpha\pi}{2}\right)}{R^2C^2} + \frac{CR \cos\left(\frac{\gamma\pi}{2}\right)}{R^2C^2} + \frac{1}{C^3R^2R_3} = 0, \quad (6a)$$

$$\frac{\omega^{\alpha+\beta+\gamma} \sin\left(\frac{(\beta+\alpha+\gamma)\pi}{2}\right) + \frac{\omega^{\beta+\alpha} \sin\left(\frac{(\beta+\alpha)\pi}{2}\right)}{CR} + \frac{\omega^{\beta+\gamma} \sin\left(\frac{(\gamma+\beta)\pi}{2}\right)}{2\omega^{\alpha+\gamma} \sin\left(\frac{(\alpha+\gamma)\pi}{2}\right) + \frac{\omega^\beta \sin\left(\frac{\beta\pi}{2}\right)}{R^2C^2} + \frac{\omega^\alpha \sin\left(\frac{\alpha\pi}{2}\right)}{R^2C^2} + \frac{\omega^\gamma \sin\left(\frac{\gamma\pi}{2}\right)}{R^2C^2} = 0. \quad (6b)$$

The condition of oscillation R_3 is calculated by first solving (6b) to get ω then substitute back in (6a) to calculate the value of R_3 . The TF between each two oscillatory outputs is very important factor in obtaining the phase difference as illustrated in Tables I and II.

A study of some special cases is introduced in this section with $C = 1.2 \times 10^{-6}$. The presented study involves five cases as follows: $\{\alpha = \beta = \gamma, (\alpha = \beta) \neq \gamma, (\alpha = \gamma) \neq \beta, (\beta = \gamma) \neq \alpha, \text{ and } (\alpha = \beta = \gamma = 1)\}$ with their oscillation frequency and condition summarized in Table III. The last investigated case is the integer case and it is considered a special case from each of

the presented ones. The first investigated case is equal order when $\alpha = \beta = \gamma$, where oscillation occurs for a specific range of α such that $(2/3) < \alpha < (4/3)$ as depicted in Fig. 4(a). The oscillation frequency range inversely proportional to both R and α while R_3 is directly proportional to them. When $\alpha = \beta \neq \gamma$, the surfaces of oscillation frequency and condition versus $\alpha - \gamma$ plane are illustrated in Fig. 4(b) with $R = 10k\Omega$. It achieves the same oscillation behavior as the case $\beta = \gamma \neq \alpha$. For the third case with $\alpha = \gamma \neq \beta$, three values of β are studied as illustrated in Fig. 4(c) where decreasing its value increases the obtained frequency range with $R = 10k\Omega$. The extra degree of freedom provided by the fractional order parameters increases the design flexibility.

From the transfer function ϕ_{32} can be related to the other two phases as mentioned in Table II. Figure 5(a) depicts the

TABLE I. TF BETWEEN EACH TWO OSCILLATORY OUTPUTS

$T_{21} = \frac{v_2}{v_1}$	$\frac{s^\alpha + \frac{1}{CR}}{1/CR}$
$T_{31} = \frac{v_3}{v_1}$	$\frac{s^{\beta+\alpha} + \frac{2s^\alpha}{CR} + \frac{s^\beta}{CR} + \frac{1}{R^2C^2}}{1/R^2C^2}$
$T_{32} = \frac{v_3}{v_2}$	$\frac{s^{\beta+\alpha} + \frac{2s^\alpha}{CR} + \frac{s^\beta}{CR} + \frac{1}{R^2C^2}}{\frac{1}{CR} \left(s^\alpha + \frac{1}{CR} \right)}$

TABLE II. PHASE DIFFERENCE BETWEEN EACH TWO OSCILLATORY OUTPUTS

ϕ_{21}	$\tan^{-1} \frac{\omega^\alpha \sin\left(\frac{\alpha\pi}{2}\right)}{\omega^\alpha \cos\left(\frac{\alpha\pi}{2}\right) + \frac{1}{CR}}$
ϕ_{31}	$\tan^{-1} \frac{\omega^{\beta+\alpha} \sin\left(\frac{(\beta+\alpha)\pi}{2}\right) + \frac{2\omega^\alpha \sin\left(\frac{\alpha\pi}{2}\right)}{CR} + \frac{\omega^\beta \sin\left(\frac{\beta\pi}{2}\right)}{CR}}{\omega^{\beta+\alpha} \cos\left(\frac{(\beta+\alpha)\pi}{2}\right) + \frac{2\omega^\alpha \cos\left(\frac{\alpha\pi}{2}\right)}{CR} + \frac{\omega^\beta \cos\left(\frac{\beta\pi}{2}\right)}{CR} + \frac{1}{R^2C^2}}$
ϕ_{32}	$\phi_{31} - \phi_{21}$

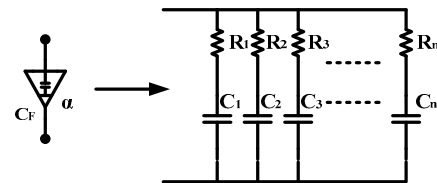


Fig. 2. Approximation the capacitor any general order $0 < \alpha < 1$.

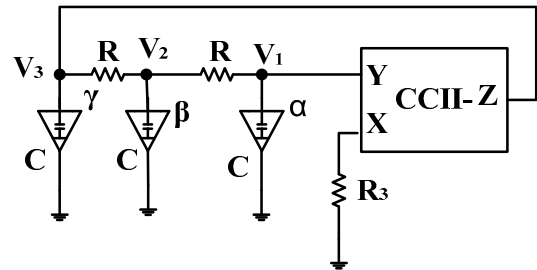


Fig. 3. Fractional-order oscillator structure.

phase versus the fractional order when $\alpha = \beta = \gamma$. Also, a contour color map for both ϕ_{21} and ϕ_{31} versus $\alpha - \gamma$ plane is illustrated in Fig. 5(b) for the case $\alpha = \beta \neq \gamma$. Figure 6 shows phase versus frequency for three different values of β with $\alpha = \gamma$ where increasing β increases the obtained phase range. The phase and frequency are shown to be completely controlled with the fractional orders.

TABLE III. SPECIAL CASES

#	(ω, R_3)
$\alpha = \beta = \gamma$	$\omega^\alpha = \frac{-2 \sin(\alpha\pi) - \sqrt{\sin^2(\alpha\pi) + 3 \sin^2(\frac{\alpha\pi}{2})}}{CR \sin(\frac{3\alpha\pi}{2})}$ $R_3 = \frac{-1}{\omega^{3\alpha} \cos(\frac{3\alpha\pi}{2}) + \frac{4\omega^{2\alpha} \cos(\alpha\pi) + 3\omega^\alpha \cos(\frac{\alpha\pi}{2})}{R^2 C^2}}$
$\alpha = \beta \neq \gamma$	$\omega^{2\alpha+\gamma} \sin\left(\frac{(2\alpha+\gamma)\pi}{2}\right) + \frac{\omega^{2\alpha} \sin(\alpha\pi)}{CR} + \frac{3\omega^{\alpha+\gamma} \sin(\frac{(\alpha+\gamma)\pi}{2})}{CR} + \frac{2\omega^\alpha \sin(\frac{\alpha\pi}{2})}{R^2 C^2} + \frac{\omega^\gamma \sin(\frac{\gamma\pi}{2})}{R^2 C^2} = 0$ $R_3 = \frac{-1}{\frac{\omega^{2\alpha+\gamma} \cos(\frac{(2\alpha+\gamma)\pi}{2}) + \frac{\omega^{2\alpha} \cos(\alpha\pi)}{CR} + \frac{3\omega^{\alpha+\gamma} \cos(\frac{(\alpha+\gamma)\pi}{2})}{CR} + \frac{2\omega^\alpha \cos(\frac{\alpha\pi}{2})}{R^2 C^2} + \frac{\omega^\gamma \cos(\frac{\gamma\pi}{2})}{R^2 C^2}}$
$\alpha = \gamma \neq \beta$	$\omega^{\beta+2\alpha} \sin\left(\frac{(\beta+2\alpha)\pi}{2}\right) + \frac{2\omega^{\beta+\alpha} \sin(\frac{(\beta+\alpha)\pi}{2})}{CR} + \frac{2\omega^{2\alpha} \sin(\alpha\pi)}{CR} + \frac{\omega^\beta \sin(\frac{\beta\pi}{2})}{R^2 C^2} + \frac{2\omega^\alpha \sin(\frac{\alpha\pi}{2})}{R^2 C^2} = 0$ $R_3 = \frac{-1}{\frac{\omega^{\beta+2\alpha} \cos(\frac{(\beta+2\alpha)\pi}{2}) + \frac{2\omega^{\beta+\alpha} \cos(\frac{(\beta+\alpha)\pi}{2})}{CR} + \frac{2\omega^{2\alpha} \cos(\alpha\pi)}{CR} + \frac{\omega^\beta \cos(\frac{\beta\pi}{2})}{R^2 C^2} + \frac{2\omega^\alpha \cos(\frac{\alpha\pi}{2})}{R^2 C^2}}$
$\beta = \gamma \neq \alpha$	$\omega^{\alpha+2\beta} \sin\left(\frac{(\alpha+2\beta)\pi}{2}\right) + \frac{3\omega^{\beta+\alpha} \sin(\frac{(\beta+\alpha)\pi}{2})}{CR} + \frac{\omega^{2\beta} \sin(\beta\pi)}{CR} + \frac{2\omega^\beta \sin(\frac{\beta\pi}{2})}{R^2 C^2} + \frac{\omega^\alpha \sin(\frac{\alpha\pi}{2})}{R^2 C^2} = 0$ $R_3 = \frac{-1}{\frac{\omega^{\alpha+2\beta} \cos(\frac{(\alpha+2\beta)\pi}{2}) + \frac{\omega^{2\beta} \cos(\beta\pi)}{CR} + \frac{3\omega^{\beta+\alpha} \cos(\frac{(\beta+\alpha)\pi}{2})}{CR} + \frac{2\omega^\beta \cos(\frac{\beta\pi}{2})}{R^2 C^2} + \frac{\omega^\alpha \cos(\frac{\alpha\pi}{2})}{R^2 C^2}}$
Inte	$\omega = \frac{\sqrt{3}}{CR}$
	$R_3 = R/12$

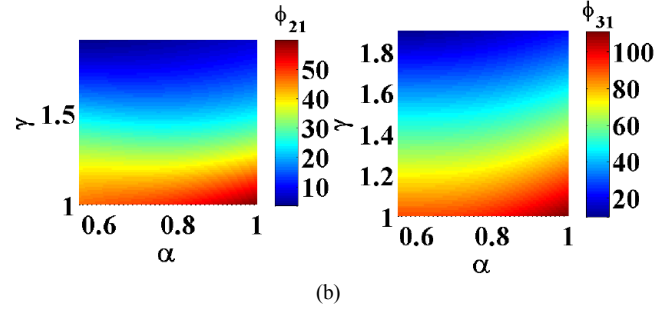
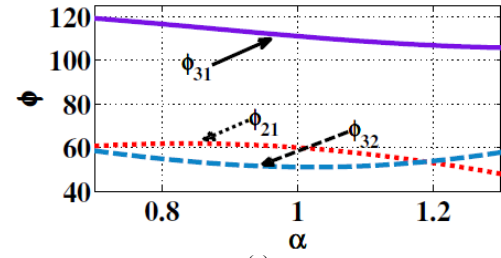


Fig. 5. Phase versus fractional order for (a) $\alpha = \beta = \gamma$, and (b) $\alpha = \beta \neq \gamma$.

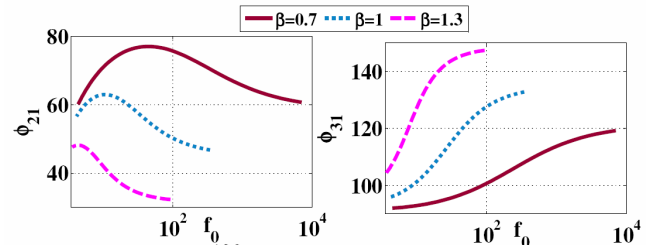


Fig. 6. Phase versus frequency with different β for $\alpha = \gamma \neq \beta$.

III. Simulation Results

In this section, Spice simulation, experimental results along with stability analysis of some cases are presented to verify the theoretical findings. The stability is a very important factor to determine the system performance and behavior where the location of the system poles determines whether the system is stable or not. In the fractional domain; to study stability in fractional order system, it is required to transform the s-plane to a more general one called W-plane which includes the fractional orders [15] then mapping back to s-plane. The simulation parameters are $C = 1.2 \times 10^{-6}$, $R = 10 \text{ k}\Omega$. The fractional order capacitor is implemented as shown in Fig. 2 where the values of the resistances, the capacitors and the number of branches depends on the order of the capacitor as presented in [13]. The first case is simulated by Spice with fractional orders, $\alpha = \gamma = 1$ & $\beta = 0.8$, and the oscillation condition R_3 is calculated according to Table III to be 367Ω . The output waveforms are depicted in Fig. 7(a) with oscillation frequency resulting from this case equals 40Hz. The THD is measured to be 4.6%. The poles for this oscillator are depicted in Fig. 7(b) in both s-plane and W-plane. Some roots exist in the non-physical region in the W-plane where there are no physical roots in the s-plane and two roots on the $j\omega$ axis so the stability of the system is guaranteed. For experimental verification; the circuit is built on NI ELVIS II series, the kit from national instrument which is connected to the computer through USB cable to measure the outputs voltages

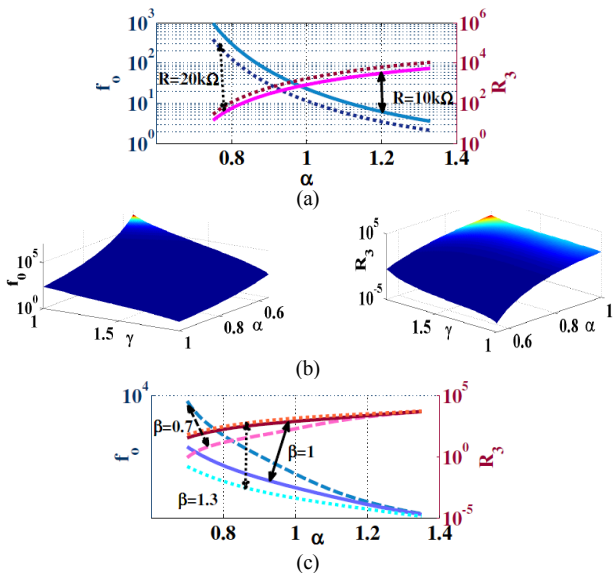


Fig. 4. Oscillation frequency and condition for (a) $\alpha = \beta = \gamma$, (b) $\alpha = \beta \neq \gamma$, and (c) $\alpha = \gamma \neq \beta$.

through the scope. The scope shows two outputs once at a time. The CCII is implemented with two AD844 as shown in Fig. 1(b). The employed fractional orders in the experimented case are $\alpha = 0.8, \beta = \gamma = 1$ with circuit components: $R = 20k\Omega$, $C = 1 \times 10^{-8}$ and The value of R_3 is calculated according to Table III and adjusted to the circuit through the potentiometer to $0.6k\Omega$ as shown in Fig. 8. The scope output V_3 & V_2 are demonstrated in Fig. 9.

IV. CONCLUSION

In this paper, a generalization for a well-known phase shift oscillator based on single CCII into the fractional-order domain was presented. The general oscillation frequency, condition and the phase difference were derived. Also, some special cases were discussed numerically and summarized in tables. The extra degree of freedom provided by the fractional order parameters proved to add more control on oscillator parameters. Finally, Spice simulations along with experimental results were presented to show the reliability of the design. Stability discussion of the simulated cases was presented.

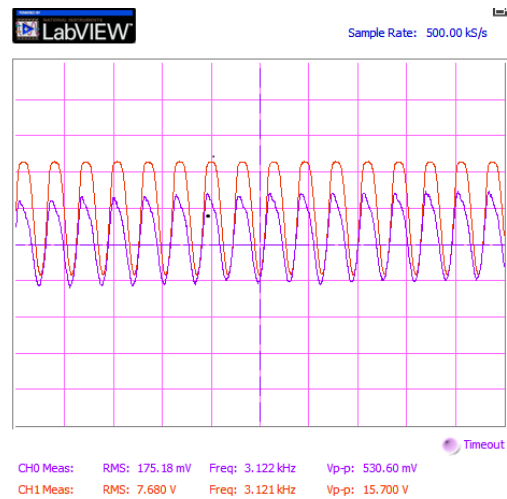


Fig. 9. Scope output V_3 & V_2 .

REFERENCES

- [1] A. S. Sedra, and K. C. Smith, "A second generation current conveyor and its applications," *IEEE Trans. Circ. Theor.*, vol. 132, pp. 132-134, 1970.
- [2] A. M. Soliman, "Simple sinusoidal active RC oscillators," *INT. J. electronics*, vol. 39, no. 4, pp. 455-458, 1975.
- [3] H. O. Elwan, and A. M. Soliman, "CMOS differential current conveyors and applications for analog VLSI", *Analog Integrated Circuits and Signal Processing*, Vol. 11, pp. 35-45, 1996.
- [4] A. M. Soliman, "Current conveyor filters: classification and review", *Micro. Electron. J.*, Vol. 29, pp. 133-149, 1998.
- [5] A. M. Soliman, "Current conveyor based or unity gain cells based two integrator loop oscillators," *Microelectron. J.* vol. 42, no. 2, pp. 239-46, 2011.
- [6] K.S. Miller, "Derivatives of non integer order," *Mathemat. Mag.*, vol. 68, no. 3, pp. 183-192, 1995.
- [7] I. Podlubny, I. Petras, B. Vinagre, P. O'leary, and L. Dorcak, "Analogue realizations of fractional-order controllers," *Nonlinear Dyn.*, vol. 29, pp. 281-296, 2002.
- [8] A. G. Radwan, A. M. Soliman, A.S. Elwakil, "Design equations for fractional-order sinusoidal oscillators: four practical circuits examples," *Int. J. Circ. Theor. Appl.*, 36, 473-492, 2008.
- [9] A. G. Radwan, A.S. Elwakil and A. M. Soliman, "Fractional-order sinusoidal oscillators: Design procedure and practical examples," *IEEE Trans. on Circuit and systems*, vol. 55, pp. 2051-2063, 2008.
- [10] L. A. Said, A. G. Radwan A. H. Madian, and A. M. Soliman, "Fractional Order Oscillators Based on Operational Transresistance Amplifiers," *Int. J. Electron Comm. (AEÜ)*, vol. 69, pp. 988-1003, 2015.
- [11] L. A. Said, A. G. Radwan A. H. Madian, and A. M. Soliman, "Fractional Order Oscillator Design Based on Two-Port Network," *Circuits, Systems, and Signal Processing (CSSP)*, 2015. DOI: 10.1007/s00034-015-0200-8.
- [12] M. Nakagava and K. Sorimachi, "Basic characteristics of a fractance device," *IEICE Trans. fundamentals*, pp. 1814-1818, 1992.
- [13] M. Sugi, Y. Hirano, Y. F. Miura and K. Saito, "Simulation of fractal immittance by analog circuits: An approach to the optimized circuits," *IEICE Trans. fundamentals*, vol. E82, no. 8, pp. 205-209, 1999.
- [14] L.A. Said, S. M. Ismail, A. G. Radwan, A. H. Madian, M. F. Abu El-Yazeed, and A. M. Soliman, "On the Optimization of Fractional Order Low Pass Filters," *Circuits, Systems, and Signal Processing (CSSP)*, 2015. DOI: 10.1007/s00034-016-0258-y.
- [15] A. G. Radwan, A. M. Soliman, A. S. Elwakil, and A. Sedeek, "On the stability of linear systems with fractional-order elements," *Chaos Solitons Fractals*, vol. 40, pp. 2317-2328, 2009.

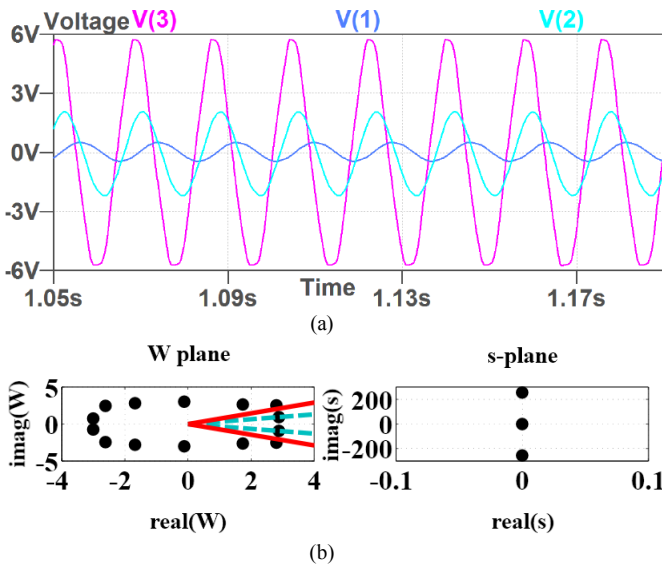


Fig. 7. For $\alpha = \gamma = 1, \beta = 0.8$. (a) Spice simulation output waveforms, and (b) system poles in s-plane and W plane.

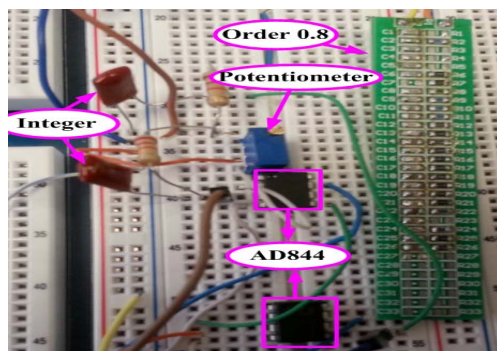


Fig. 8. The case with $\alpha = 0.8, \beta = \gamma = 1$, circuit implementation.